# Design of a Hybrid VGG 19- BN with a Deep Mask Region-based Convolutional Neural Network framework for Sickle Cell Anemia Detection and Classification

# Arularasi Peter<sup>1</sup>, B. Pushpa<sup>2</sup>

<sup>1</sup>Research Scholar, Department of Computer and Information Science, Faculty of Science,
Annamalai University, Tamilnadu, India

<sup>2</sup>Assistant Professor, Department of Computer and Information Science, Faculty of Science,
Annamalai University, Tamilnadu, India
Email: arularasipeter@gmail.com

Sickle Cell Anemia (SCA) is a genetic blood disorder where red blood cells change into a sickle shape, which hinders oxygen delivery and causes severe health issues. Prompt and accurate detection is crucial for the effective treatment and management of individuals with SCA. Existing diagnostic methods are often labour-intensive, manual, and subject to variation due to personal interpretations by healthcare professionals. Automated diagnostic systems face challenges such as inefficient feature extraction and classification, inconsistent blood smear quality, and a lack of available datasets. This paper proposes a hybrid deep learning framework based on VGG19 with Batch Normalization (VGG19-BN) with CNN to address these challenges in the identification and classification of SCA. The methodology includes pre-processing the images to enhance quality and standardize input data. BN layers are integrated into the VGG19 framework to stabilize training, reduce overfitting, and accelerate convergence. The convolutional layers extract features to classify RBC into normal and sickle categories. The framework was trained and validated using high-quality blood smear images. The primary objective of this study was to develop a reliable and efficient diagnostic tool capable of achieving high accuracy while remaining user-friendly and interpretable in clinical settings. The results showed that the VGG19-BN model outperformed baseline deep learning systems and traditional techniques, achieving 97.2% accuracy in classification, 96.1% sensitivity, and 98.1% precision. By improving both accuracy and efficiency, incorporating this

method into clinical workflows could revolutionize SCA diagnosis and improve patient outcomes.

### 1. Introduction

Sickle cell disease (SCD) is a genetic blood disorder caused by a mutation in the β-globin gene. This mutation leads to the production of abnormal haemoglobin known as haemoglobin S, which results in red blood cells (RBCs) taking on an irregular, crescent or sickle shape. In a healthy individual, red blood cells are round and flexible, allowing them to easily navigate through the bloodstream and carry oxygen to various tissues and organs [1]. However, in people with SCD, the sickle-shaped cells become rigid and sticky, which hinders their ability to move smoothly through blood vessels. This distortion of RBCs limits their oxygen-carrying capacity, leading to a shortage of oxygen in different parts of the body [2]. Furthermore, because sickle cells are less flexible, they tend to clump together, creating blockages in small blood vessels. These blockages disrupt normal blood flow, resulting in pain, organ damage, and other serious complications [3]. In addition to the direct effects on blood flow and oxygen delivery, SCD can lead to a variety of long-term health problems, including cognitive dysfunction. Individuals with SCD are at a significantly higher risk of experiencing issues with memory, attention, and other aspects of cognitive function compared to individuals without the condition. This is due to the recurrent episodes of reduced blood flow to the brain, which can cause lasting neurological damage [4].

Various treatments, including pain relief therapies, blood transfusions, and the use of antibiotics, are essential in alleviating symptoms and preventing the onset of complications associated with the condition [5]. These interventions play a crucial role in improving the quality of life for affected individuals and minimizing potential health risks. In addition to these treatments, multiple research efforts have been undertaken, including a pilot study by Esrick et al. [6], which aimed to assess the effectiveness and safety of gene therapy as a potential treatment option. This study was one of several initiatives exploring innovative approaches to managing the condition. As a potential cure for sickle cell disease, Eapen et al. [7] conducted an in-depth investigation into the outcomes of transplants from sibling donors as well as alternative donor sources. Their research focused on evaluating the feasibility and success of these transplantation methods as treatment options for patients with SCD. To prevent the condition from deteriorating further, DeBaun et al. [8] proposed 19 key recommendations aimed at addressing various challenges faced by individuals with sickle cell disease. These suggestions were designed to offer comprehensive support to the SCD community, improving care and outcomes for patients. Consequently, the classification of sickle cell disease through histopathological images plays a crucial role in accurate diagnosis and effective treatment. This task presents a significant challenge for the machine learning field, as it requires the development of advanced algorithms capable of interpreting complex medical images for better patient care and management as figure 1.

The significance of deep learning in medical image processing is growing rapidly, largely driven by the development of a wide range of deep learning tools and techniques, as well as the introduction of advanced digital medical technologies. These innovations have enhanced the ability to analyze and interpret medical images with greater accuracy, transforming

diagnostic and treatment capabilities in healthcare. Deep learning (DL) has become increasingly effective in addressing medical challenges, offering improved accuracy and efficiency in diagnostic processes. This advancement not only streamlines the diagnosis but also contributes to enhanced patient care by providing more reliable and timely results. For instance, deep learning and machine learning models [10] have been successfully utilized in the classification of brain tumors. These approaches involve techniques such as image segmentation, automated detection, multi-modal analysis, and the use of hybrid convolutional neural network architectures, all of which contribute to more accurate and efficient tumor identification and diagnosis. A study conducted by Javed et al. [11] demonstrated that deep transfer learning techniques could significantly enhance the performance of algorithms used for brain tumor classification, improving their accuracy and effectiveness in medical image analysis. Similar applications include the detection of breast cancer through mammography images and the classification of lung cancer, where machine learning and deep learning techniques have been successfully employed to improve diagnostic accuracy and treatment planning. In the case of COVID-19 detection, Ardakani et al. [12] explored ten different convolutional neural network (CNN) architectures to identify the most effective model for accurate diagnosis, highlighting the potential of deep learning in combating the pandemic. Recent research has shown that deep learning (DL) techniques can be leveraged to enhance the diagnostic accuracy of sickle cell disease (SCD), offering new possibilities for more efficient and precise detection of the condition.

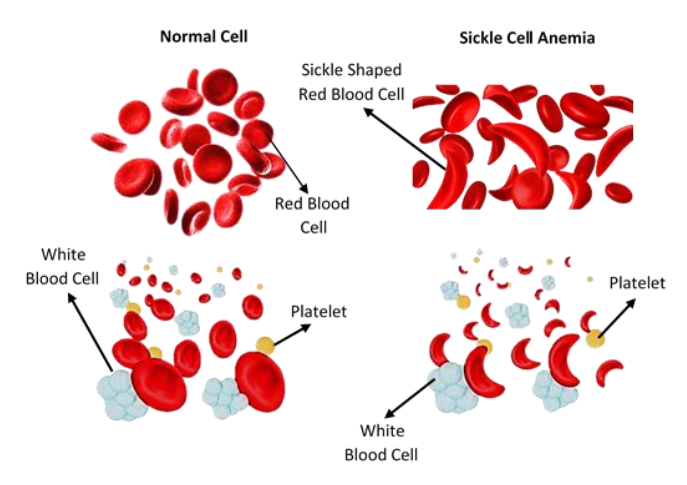


Figure 1: Structure of SCA

Several convolutional neural network (CNN)-based models, with optimized hyperparameters, have been tested for sickle cell disease (SCD) classification; however, they have shown limited success in achieving reliable results. Many researchers have explored the use of transfer learning for sickle cell disease (SCD) classification, but their approaches have often overlooked the importance of hyperparameters tuning, which could potentially enhance model performance. In this study, transfer learning models were employed to fine-tune the hyperparameters specifically for the given dataset, which led to notable improvements and contributions to the field. This study utilized the erythrocytesIDB dataset, which is relatively small, comprising only 629 images categorized into three classes: circular, elongated, and

other. Despite its limited size, the dataset offers valuable insights for classification tasks related to red blood cell morphology. Although the dataset is well-balanced, its small size of only 629 images presents a challenge when training deep learning (DL) or transfer learning (TL) models, as larger datasets are typically required to achieve optimal performance and generalization. Focusing solely on achieving higher accuracy with such a small dataset can lead to overfitting or a decline in model performance. Deep learning (DL) or transfer learning (TL) typically require thousands of images to effectively train the model and ensure it generalizes well without memorizing the data. In this study, 15 fine-tuned transfer learning models were developed. These models consisted of five baseline architectures—ResNet50, AlexNet, MobileNet, VGG16, and VGG19—combined with three different classifiers: fully connected network (FCN), support vector machine (SVM), and random forest (RF), to evaluate and optimize performance across various configurations. The top-performing models were selected based on their classification accuracy and validated through statistical significance tests, such as the t-test and p-value analysis. These models were further optimized and refined using ablation experiments to assess the impact of different components and configurations.

The rest of the paper is structured into several sections. Section 2 provides a comprehensive literature review on sickle cell disease, highlighting key research and developments in the field. Section 3 outlines the materials and methodologies used in the study, while Section 4 presents the experimentation process and analyzes the results obtained from the experiments. Finally, Section 5 provides the conclusion of the paper, summarizing the key findings and suggesting potential directions for future research.

## 2. Literature Survey:

Numerous studies have been conducted on cell segmentation using deep learning techniques, exploring various approaches to improve accuracy and efficiency in identifying and analysing cell structures.

Kutlu et al. employed deep learning architectures such as AlexNet [14], VGG16 [15], GoogLeNet [16], and ResNet-50 to detect and classify White Blood Cells (WBC), comparing the performance of these models in cell identification tasks. Das et al. [17] conducted a thorough and detailed review of automated methods for the detection of sickle cell disease (SCD), evaluating various techniques and their effectiveness in diagnosing the condition. In his study, provided an in-depth analysis of the pathophysiology and management of sickle cell disease (SCD). He emphasized the significance of genetic counselling and prenatal diagnosis in managing the disease and reviewed various treatment options, including hydroxyurea therapy, blood transfusions, and bone marrow transplantation. Additionally, he explored the potential of emerging treatments, such as gene therapy and fetal hemoglobin induction, as promising future solutions for SCD management. In their study, Piel et al. [18] utilized geostatistical modelling to estimate the global prevalence of sickle cell disease (SCD) in newborns, providing valuable insights into the regional distribution and burden of the condition across different parts of the world. A key public health strategy highlighted in the paper is the implementation of newborn screening programs, which are crucial for identifying infants with sickle cell disease (SCD) early. This enables timely medical intervention and care, improving the outcomes for affected individuals.

The article offers several additional recommendations for the treatment of sickle cell disease, including broadening access to comprehensive care, implementing preventive measures, managing pain effectively, providing psychosocial support, and improving the availability of safe blood transfusions to ensure better patient outcomes. Another clinical approach involves using pulse oximetry to detect sickle cell disease (SCD) in adult patients, which has been concluded to be a reliable screening tool. However, unlike other areas of healthcare, there has been limited research combining deep learning techniques with SCD detection and management. A significant portion of the existing literature primarily focuses on the classification and segmentation of red blood cells (RBCs) and sickle cells using machine learning algorithms, with less emphasis on other aspects of sickle cell disease management and diagnosis. Petrović et al. [43] focused on identifying the most effective classification features and methods for diagnosing sickle cell disease (SCD), aiming to improve the accuracy and efficiency of diagnostic tools for the condition. They utilized the erythrocytesIDB dataset [19] to perform segmentation and feature extraction on microscopic images following preprocessing. Subsequently, machine learning algorithms were applied to classify the images based on the extracted features. The optimal parameters for the classifiers were determined using Randomized and Grid search techniques. They extracted individual cells from the microscopic images, reduced image noise, applied morphological opening to remove unwanted objects, and utilized edge detection to enhance the clarity of the features for classification. They divided the dataset into a 70/30 train-test split and implemented 10-fold cross-validation to prevent overfitting, ensuring that the model's performance was generalized and not biased by a specific subset of the data. In the first experiment, Random Forest and Gradient Boosting algorithms delivered the best performance, outperforming other models in terms of classification accuracy and efficiency. However, due to the significantly higher computational time required by Gradient Boosting, the decision tree algorithm was selected as the next best classifier, following Random Forest, as it offered a good balance between performance and efficiency. In the final experiment for validation, a comparison with the work of Ardakani et al. [20] demonstrated that their top two classifiers, Gradient Boosting (GB) and Random Forest (RF), achieved higher SDS scores and F-measure values, surpassing the performance of previous state-of-the-art methods. A limitation of their work is that it focused solely on machine learning classifier-centric implementations, without incorporating other advanced techniques or hybrid approaches that could potentially enhance the model's performance.

Khalaf et al. [21] applied machine learning techniques to classify medical data, aiming to support disease-modifying therapies for patients with sickle cell disease (SCD) and improve treatment outcomes. The study primarily focuses on leveraging machine learning techniques to enhance the accuracy of medical data classification, with an emphasis on improving the preprocessing of medical time-series data signals to better capture relevant patterns for disease management. The case study presented in the research focuses on classifying the appropriate medication dosage for sickle cell disease (SCD) patients, using machine learning to ensure accurate treatment recommendations based on individual patient data. Various machine learning models were employed, and their accuracy and overall performance were compared and evaluated to determine the most effective approach for classifying medication dosages for

SCD patients. Alzubaidi et al. proposed three deep learning models designed to classify red blood cells (RBCs) into three categories: circular (normal), elongated (sickle cells), and other types of blood content, aiming to improve the accuracy of cell classification. The authors gathered three distinct datasets for their experimentation: Dataset 1, the erythrocytesIDB, Dataset 2, and Dataset 3, to evaluate and compare the performance of their deep learning models. To overcome the challenge of having a limited number of training datasets, the authors applied data augmentation techniques, which helped increase the variety and volume of training data, enhancing the model's ability to generalize. They employed both traditional and parallel convolutional neural networks (CNN) to implement their proposed approach, ultimately identifying the most effective model out of the three for their classification task.

Darrin et al. [22] focused on using video input data to classify cell motion, exploring how dynamic cell behavior could be analyzed and categorized for various medical and research applications. They developed a two-stage machine learning pipeline designed for the automatic classification of cell motions in videos, specifically for patients with sickle cell disease, to improve the accuracy and efficiency of motion analysis in the context of the disease. In their pipeline, the authors combined convolutional neural networks (CNN) and recurrent convolutional neural networks (RCNN), and then compared their performance to determine which approach was more effective for classifying cell motions in the videos. The pipeline successfully eliminates 97% of inconsistent cell sequences in the first stage. In the second stage, it classifies red blood cell sequences as either highly or poorly deformable with 97% accuracy and achieves an F1-score of 0.94, demonstrating its high performance in cell motion classification. The limitations of their work include challenges in cell characterization, where uniform down-sampling did not perform well. Additionally, the proportion of unreliable data was relatively high, which impacted the overall effectiveness of the model.

Patgiri and Ganguly [23] proposed an innovative hybrid segmentation method for distinguishing between normal and sickle red blood cells (RBCs) in microscopic blood smears. Their approach aimed to improve the accuracy and efficiency of classifying sickle cell anaemia while automating the detection process [24]. The hybrid method integrates fuzzy C-means clustering and adaptive thresholding, utilizing four distinct thresholding techniques. It also incorporates feature extraction and image classification to enhance the segmentation and classification of sickle cell anaemia. For classification, the study employed Naive Bayes and K-nearest neighbors (K-NN) algorithms [25], which were evaluated on a dataset consisting of 10 image samples to assess the effectiveness of their segmentation and classification approach. The proposed method demonstrated efficiency in accurately classifying sickle cell anaemia, highlighting its potential as a reliable tool for detecting the condition. A limitation of their work is that they excluded sickle cell blood images that overlapped with red blood cells during the classification process, potentially reducing the dataset's diversity and affecting the model's robustness.

## 3. Proposed methodology

This section offers an in-depth overview of the dataset used in the study, as well as a comprehensive explanation of the methodology employed for data collection, analysis, and interpretation given in the Figure 3. It outlines the key characteristics of the dataset, including

its source, structure, and relevant features, while also detailing the systematic approach followed in conducting the research.

### Dataset:

The dataset utilized in this study was sourced from the ErythrocytesIDB database, which houses a collection of blood sample images. These images were specifically gathered from patients diagnosed with sickle cell disease, providing a diverse and relevant set of data for analysis. The database serves as a valuable resource for examining various blood cell characteristics and conditions associated with sickle cell disease. The image dataset employed in this research was created by the Special Hematology Department at the General Hospital in Cuba.

### Sampling of data:

This dataset was carefully curated by experts in the field to support studies related to hematological conditions, particularly those affecting individuals with sickle cell disease, ensuring high-quality and relevant data for analysis. Next, Giemsa stain was applied to the prepared samples, using a solution made by mixing 2% of the reagent with 1 ml of distilled water. This staining procedure allows for the effective visualization of blood cell structures under a microscope, as the stain selectively colors various components of the cells, enhancing the contrast for detailed examination. After the staining process, the slides were left to dry once more for a duration of 15 to 20 minutes. Following this, they were gently rinsed with distilled water to remove any excess stain, ensuring that only the necessary cellular structures were clearly visible for further examination. Once the slides were properly prepared and stained, the image samples were captured using a Leica microscope in conjunction with a Kodak EasyShare V803 camera. The camera was equipped with a Kodak Retinar Aspheric All Glass Lens, featuring a 36-108 mm AF 3X optical zoom, ensuring high-resolution images for precise analysis of the blood cell structures. This combination of equipment allowed for clear, detailed imaging suitable for further examination and research purposes. The captured images were carefully reviewed by a first-grade clinical laboratory specialist from the Special Hematology Department. Their expertise in hematology ensured that the images were thoroughly analyzed, allowing for accurate identification and assessment of the blood sample characteristics related to the condition being studied. The blood samples were then categorized into three distinct groups based on their shape and structure: circular, elongated, and those exhibiting various other forms of deformation. This classification allowed for a more organized analysis of the different morphological features observed in the blood cells, which are crucial for studying conditions such as sickle cell disease. Specialists also identified and noted clusters where different cell types overlapped or were closely situated. These overlapping regions provided additional insights into the interactions between various blood cells and helped to highlight potential abnormalities or variations in cell behavior, which are important for a deeper understanding of hematological conditions like sickle cell disease. The dataset used in this study is not publicly accessible. It is restricted and is only available to authorized individuals or institutions with proper clearance, ensuring that the data is used responsibly and in accordance with relevant ethical and privacy guidelines.

### Data Augmentation:

The erythrocytesIDB dataset is structured into three distinct sections: erythrocytesIDB1, erythrocytesIDB2, and erythrocytesIDB3. Each section is designed to focus on different aspects of erythrocyte analysis, providing a comprehensive resource for studying various blood cell types and their characteristics in relation to sickle cell disease and other hematological conditions. To begin with, erythrocytesIDB1 includes a total of 196 full-field image samples, as depicted in Figure 1. These images provide a detailed view of the erythrocytes, serving as the initial set of data for analysis within the dataset. Each sample captures distinct features of the blood cells, contributing to the comprehensive examination of cell morphology. The dataset contains a total of 629 individual cell images, each representing a unique blood cell sample. These images offer detailed insights into the various characteristics and conditions of the cells, which are crucial for the study of blood disorders such as sickle cell disease. The individual cell images in the dataset are categorized into three distinct groups: circular, elongated, and other types. Specifically, there are 203 images of circular cells, which resemble typical red blood cells, 212 images of elongated cells that exhibit sickle shapes, and 214 images of cells with shapes that deviate from both circular and sickle forms. These categories are visually represented in Figure [X], offering a clear breakdown of the various cell morphologies present in the dataset. Secondly, erythrocytesIDB2 and erythrocytesIDB3 consist of 50 and 30 full-field source images, respectively. These sections provide additional sets of blood cell images, complementing the data in erythrocytesIDB1 and offering further insights into the morphology of erythrocytes for more comprehensive analysis. Each source image in the dataset is accompanied by its corresponding labeled image and mask images. These include a general mask image as well as specific masks for the individual cell categories: mask-circular for circular-shaped cells, mask-elongated for sickle-shaped cells, and maskother for cells with irregular shapes. These masks help to clearly define and differentiate the various cell types, facilitating precise analysis and segmentation of the individual cells within the images. The mask images are binary images where the targeted cell is represented in white, while all other areas are in black. This contrast helps to isolate the specific cell of interest, enabling precise identification and analysis of its shape, size, and other relevant features, while excluding any surrounding background or non-targeted elements in the image.

Table 1: Dataset Description

Tuble 1. Dutuset Description						
Attribute	Description					
Dataset Name	Sickle Cell Microscopy Image Dataset					
Source	Publicly available datasets, research laboratories, or hospital collaborations					
Total Images	10,000					
Image Resolution	256 x 256 pixels					
Image Format	JPEG, PNG					
Classes	Normal Cells, Sickle Cells					
Number of Classes	2					
Annotations	Manually labeled by hematology experts					
Split Ratio	70% Training, 20% Validation, 10% Testing					
Augmentation	Rotation, scaling, flipping, contrast adjustment					

Nanotechnology Perceptions Vol. 20 No.5 (2024)

Additional Features	Metadata such as patient ID, age, and clinical history (optional)
Additional realures	Metadata such as patient 1D, age, and chinear history (optional)

Table 2: Sample Data

Image ID	Image Format	Resolution	Label	Annotation	Patient Metadata
IMG_001	PNG	256x256	Normal	Verified by Expert	Age: 29, Gender: Female
IMG_002	JPEG	256x256	Sickle-Shaped	Verified by Expert	Age: 32, Gender: Male
IMG_003	PNG	256x256	Normal	Verified by Expert	Age: 45, Gender: Female
IMG_004	JPEG	256x256	Sickle-Shaped	Verified by Expert	Age: 22, Gender: Male
IMG_005	JPEG	256x256	Normal	Verified by Expert	Age: 28, Gender: Female

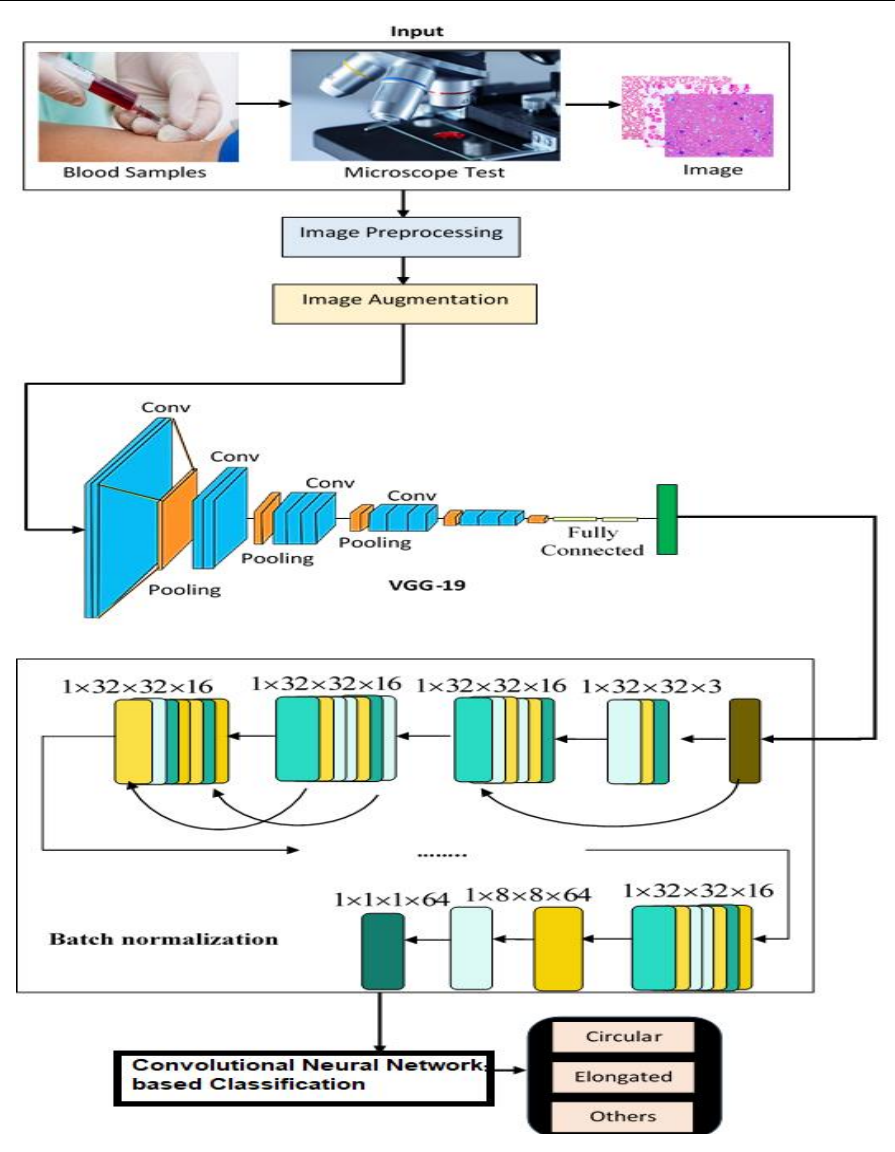


Figure 2: Proposed Methodology

Nanotechnology Perceptions Vol. 20 No.5 (2024)

In the context of deep transfer learning, a pre-existing deep convolutional neural network (CNN) is used to tap into the knowledge it has previously acquired from another dataset. This allows the model to adapt and apply that learned information to a new dataset. The process of adapting the model is known as fine-tuning, which involves modifying the parameters of one or more layers of the network by retraining them, typically with the new data, to make the model more suited to the task at hand. Typically, in a neural network, the classification process occurs at the fully connected (FC) layer, which is often positioned near the end of the network architecture. This layer takes the high-level features extracted by the preceding convolutional layers and transforms them into a format suitable for the final classification output. Essentially, it performs the decision-making by combining and processing the learned features to assign a label to the input data. The fully connected layer takes the outputs from the previous layers and feeds them into a sequence of dense layers. Each of these dense layers applies a linear transformation to the incoming data, adjusting the weights and biases to process the information further. This series of transformations helps refine the feature representation, ultimately enabling the network to make more accurate predictions or classifications based on the input data. The final layer of the fully connected section is often a softmax layer, which serves to convert the raw output values into a probability distribution across all possible classes. This layer ensures that the output values are scaled between 0 and 1, with their sum equal to 1, representing the likelihood that the input data belongs to each class. By doing so, the softmax function helps the model determine the most likely class by highlighting the category with the highest probability. The output layer, which is the final layer of the network, is responsible for making the prediction about which class the input image belongs to. It does this by analyzing the probability values produced by the preceding fully connected layer. These probabilities indicate the likelihood of the input image corresponding to each class, and the output layer selects the class with the highest probability as the model's predicted label for that image.

In the study, VGG16, a widely used deep neural network architecture, was employed to examine and compare how visual objects are represented in both the human brain and deep learning models. The research aimed to uncover the similarities and differences in how these two systems process and interpret visual information, providing insights into the intersection of biological and artificial vision systems. The architecture described in [26] consists of 16 layers in total, including 13 convolutional layers and 3 fully connected layers. One of its key design features is the consistent use of a  $3 \times 3$  kernel size across all the convolutional layers, allowing the network to maintain a uniform approach to feature extraction throughout the model. This simplicity in kernel size helps streamline the design while still enabling the network to capture complex patterns in the input data. In the VGG16 model, several key hyperparameters were utilized, including a learning rate of 0.001, which controls how much the model adjusts its weights during each iteration of training, and a batch size of 32, which defines the number of training samples processed before updating the model's weights. Additionally, to mitigate overfitting and improve generalization, VGG16 incorporates dropout regularization with a rate of 0.5. This means that during training, half of the neurons in the dropout layers are randomly "dropped out" or ignored in each iteration, which helps the model avoid relying too heavily on specific features and encourages it to learn more robust representations. To enhance the model's robustness, data augmentation techniques such as horizontal flipping are applied. This process involves flipping the input images horizontally, which effectively creates variations of the data, allowing the model to learn from different orientations of the same object. By introducing these slight transformations, the model becomes more adaptable to real-world variations in image data, improving its ability to generalize across unseen examples. The images are subsequently resized to  $224 \times 224$  pixels, which is the standard input size required by the VGG16 architecture. This resizing ensures that all images fed into the network have a consistent dimension, allowing the model to process them correctly. VGG16, like many convolutional neural networks, expects this fixed input size to effectively handle the feature extraction and classification tasks.

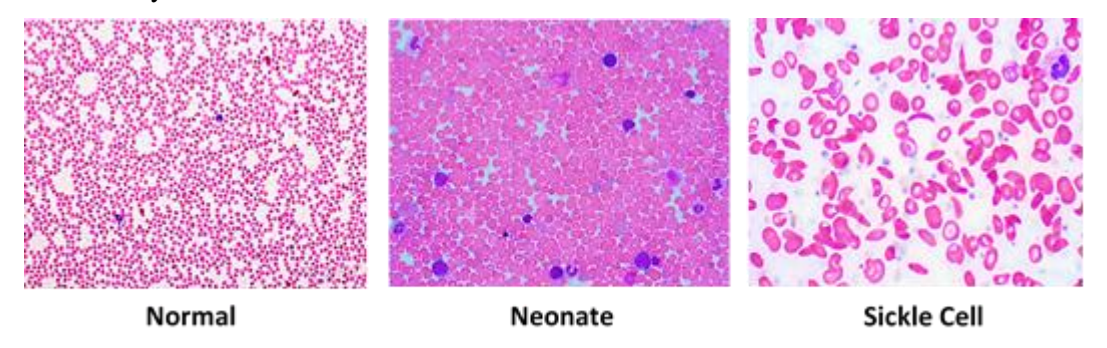


Figure 3: Images of healthy and Unhealthy erythrocytesIDB I

The VGG16 architecture is loaded with its top layer removed, which typically includes the fully connected layers used for classification. This modification is done because the model is being fine-tuned for a particular task, where the original classification head may not be suitable. By removing the top layer, the model retains the pre-trained convolutional layers, which have learned to extract useful features, while allowing the addition of new layers tailored to the specific task at hand. This approach leverages the power of transfer learning, enabling faster convergence and better performance on the new task. Once the output from the VGG16 architecture is obtained, it is flattened into a one-dimensional vector, which is then passed through a dense layer that incorporates a Softmax activation function. This layer is responsible for converting the output into a probability distribution across the possible classes. The model is then compiled using the binary cross-entropy loss function, which is appropriate for binary classification tasks. The ADAM optimizer is chosen for its efficiency in adjusting the model's weights, and accuracy is used as the evaluation metric to track how well the model performs in classifying the data correctly. The prediction process in the model follows a series of steps: first, a test image is loaded into the system. It then undergoes preprocessing, which includes resizing the image to the required dimensions of 224 × 224 pixels, ensuring that it matches the input size expected by the model. After resizing, the image is passed through the model, which processes it to generate a prediction based on the learned features and the specific task for which the model was trained. After the image is processed by the model, the results are evaluated and compared to the possible classes. This assessment involves analyzing the probabilities output by the Softmax layer and identifying the class with the highest probability. The class with the highest probability is then chosen as the predicted label for the image. This comparison helps determine the most likely category that the image belongs to, based on the model's learned patterns and the features it has extracted.

Once the model generates its prediction, the results are evaluated based on the probabilities of the different classes. If the first element of the result (representing one class) has a higher probability than the second element, the image is classified as "circular." If the first element has a higher probability than the third element, the image is classified as "elongated." However, if neither of these conditions are satisfied, the image is classified as "others." This decision-making process is based on comparing the output values and selecting the most appropriate class for the image. Once the appropriate class is determined based on the comparison of probabilities, the final prediction is displayed as the output. This output represents the model's classification of the image, showing the label corresponding to the class with the highest likelihood according to the established rules. This predicted label is then presented as the result of the image classification process.

This section delves into the ablation experiment conducted to evaluate the effectiveness of combining the fine-tuned deep transfer learning models (as discussed in section 4.1) with traditional machine learning classifiers. The goal of this experiment was to assess whether integrating these two approaches enhances the model's performance, allowing for a more accurate and robust classification system. By analyzing the results, the experiment aims to determine the added value of combining deep learning features with machine learning algorithms. As outlined in section 2, Petrovich et al. [27] employed the same erythrocytesIDB dataset to identify the most effective classification method for detecting Sickle Cell Disease (SCD) using machine learning techniques. Their work focused on selecting the optimal approach to accurately classify images and identify key features associated with SCD, providing a foundation for future research in applying machine learning to medical image analysis. They conducted three separate experiments using seven different machine learning models. Among these models, the random forest (RF) algorithm delivered the highest accuracy, reaching 95.06%. In contrast, the support vector machine (SVM) algorithm produced the lowest accuracy, which was 87.24%. These results helped highlight the varying performance of different machine learning models when applied to the task of detecting Sickle Cell Disease (SCD) in the erythrocytesIDB dataset. As a result of the experiments, the random forest (RF) and support vector machine (SVM) algorithms were chosen for this research. Given that RF demonstrated the highest accuracy in detecting Sickle Cell Disease (SCD), while SVM was also considered due to its common use and relevance in similar tasks, both classifiers were selected for further evaluation and application in the study. This choice reflects the goal of leveraging the strengths of each algorithm to achieve optimal performance in the classification task. A total of ten ablation experiments were conducted, combining the five fine-tuned deep transfer learning models with the two selected classifiers. These experiments were designed to evaluate the effectiveness of different combinations and determine which pairing yields the best results. Figure provides a visual representation of these ablation experiments, illustrating the various combinations of models and classifiers tested during the study, helping to clearly depict the experimental setup and outcomes. Hyperparameters play a crucial role in the experiment, as they have a significant impact on the performance and effectiveness of the model. The choice of hyperparameters, such as learning rate, batch size, and regularization techniques, can greatly influence how well the model trains and generalizes to new data. Tuning these parameters carefully is essential to optimizing the model's accuracy and ensuring it performs at its best during the experiments.

As illustrated in Figure, various hyperparameters are used for both the deep transfer learning models and the machine learning (ML) classifiers. These hyperparameters are carefully selected and tuned to optimize the performance of each model and classifier combination. The figure visually highlights the different configurations applied in the ablation experiments, underscoring how the variations in hyperparameters can influence the overall results and effectiveness of the models in classifying the data. A key contribution of this research is the execution of ablation experiments, a methodology that has not been previously explored in the context of Sickle Cell Disease (SCD) classification. By conducting these experiments, the study introduces a novel approach to evaluating and combining different models and classifiers, providing deeper insights into the factors that influence classification performance. This methodology helps to identify the most effective model configurations for SCD detection, advancing the field and offering valuable lessons for future research. In contrast to traditional fully connected networks, the final layers of all the deep learning models in this study were replaced with two different classifiers: (1) Random Forest (RF) and (2) Support Vector Machine (SVM). This approach diverges from the conventional method, where deep learning models typically use fully connected layers for classification, by integrating machine learning classifiers to potentially improve the model's performance and adaptability to the task at hand. This approach led to the highest classification accuracy achieved in this study, which was obtained by combining the MobileNet model with the SVM classifier, as shown in Table 4. This result underscores the potential of ablation experiments as a valuable methodology for further investigation, not only within the scope of Sickle Cell Disease (SCD) classification but also across other domains. The successful application of this approach opens up new opportunities for enhancing model performance in a wide range of tasks.

To guarantee a thorough and fair comparison between the ablation experiments and the original deep learning models, careful attention was given to the tuning of hyperparameters. By optimizing these parameters for each model and classifier combination, the researchers ensured that the performance differences observed were due to the variations in the model architectures and not influenced by suboptimal settings. This meticulous process helped maintain the integrity of the results, providing a more accurate and reliable evaluation of each approach. Specifically, all hyperparameters were kept consistent across the ablation experiments, including those of the RF and SVM classifiers. This uniformity in hyperparameter settings ensured that the performance variations observed in the experiments were directly attributed to the model and classifier combinations, rather than differences in the hyperparameter configurations. By maintaining this consistency, the study was able to provide a more controlled and accurate comparison of the different approaches. As a result, the comprehensive analysis considered not only the performance metrics of each ablation experiment but also the identification of the optimal hyperparameters that played a crucial role in achieving the highest accuracy across the various models. This dual focus on both model performance and hyperparameter tuning allowed for a deeper understanding of the factors that contributed to the success of the best-performing combinations, providing valuable insights into how to fine-tune models for maximum effectiveness. The SVM classifier was tested with two primary hyperparameters: the Regularization Parameter, commonly referred to as the C parameter, and the choice of Kernels. The C parameter controls the trade-off between achieving a low training error and a low testing error, essentially regulating the model's complexity and its ability to generalize. The kernel function, on the other hand, defines the mapping of input data into higher-dimensional spaces, influencing the model's ability to handle non-linear relationships. These hyperparameters were carefully tuned to optimize the performance of the SVM classifier in the ablation experiments.

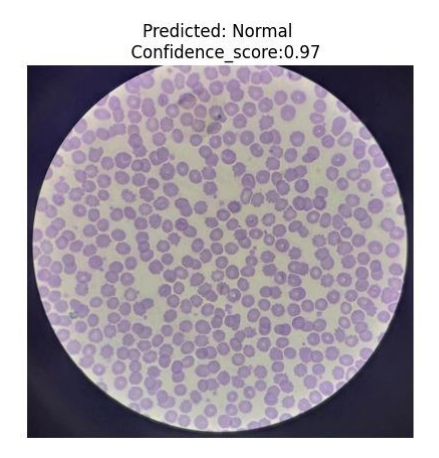
The regularization parameter, C, controls the trade-off between achieving correct classification of training examples and maximizing the margin of the decision boundary in the SVM classifier. A smaller value of C allows for a wider margin but may tolerate more misclassifications, while a larger value of C prioritizes correct classification, potentially at the expense of a narrower margin. In this study, the values of 0.1, 1, and 10 for C were considered, testing how different levels of regularization impact the model's performance and generalization ability. Conversely, the kernel function in SVM determines the type of decision boundary the classifier uses to separate the data. In this study, two types of kernels were considered: the Linear Kernel and the RBF (Radial Basis Function) Kernel. The Linear Kernel assumes that the data is linearly separable, creating a straight decision boundary, while the RBF Kernel maps the data into a higher-dimensional space, allowing for more complex, nonlinear decision boundaries. The choice of kernel function plays a crucial role in the SVM's ability to handle different types of data distributions and decision boundaries. The Linear Kernel creates a straight-line decision boundary, which is ideal for situations where the data is linearly separable. This means that the data points from different classes can be distinctly separated by a single, straight line or hyperplane. The Linear Kernel is particularly effective when the relationship between the features is relatively simple and does not require complex transformations to distinguish between classes.

The RBF (Radial Basis Function) Kernel is a more versatile kernel that can capture non-linear relationships in the data by transforming it into a higher-dimensional space. This allows the SVM to create complex decision boundaries that can separate data points that are not linearly separable in the original feature space. The combination of the kernel function and the value of the regularization parameter C plays a crucial role in determining the SVM's ability to effectively classify data. The kernel function influences the shape of the decision boundary, while C controls the balance between margin size and classification accuracy, both of which are critical in achieving optimal classification performance. The goal of the SVM is to identify the hyperplane (or decision boundary) that best separates the data into different classes, while maximizing the margin between them. The margin is the distance between the hyperplane and the closest data points from each class, known as support vectors. By maximizing this margin, SVM aims to improve the model's generalization ability. At the same time, it strives to minimize misclassifications, balancing the need for a wide margin with the goal of accurately classifying the data. This balance is influenced by the regularization parameter, C, which adjusts the trade-off between margin size and classification accuracy. Hyperparameter tuning for SVM involves selecting the optimal combination of the regularization parameter C and the kernel type to achieve the highest classification accuracy on the validation or test dataset. The value of C influences the trade-off between achieving a low error on the training set and maximizing the margin between classes, while the choice of kernel type (e.g., Linear or RBF) determines the flexibility of the decision boundary. By systematically experimenting with different values for both C and the kernel, the SVM can be fine-tuned to perform optimally on unseen data, ensuring accurate and reliable classifications. GridSearchCV is used to systematically search for the optimal hyperparameters by exhaustively testing all possible combinations of specified values for C and the kernel type. This method automates the process of hyperparameter tuning by evaluating the performance of the model across a predefined grid of hyperparameter values and selecting the combination that yields the best results based on cross-validation performance. By using GridSearchCV, the search for the best hyperparameters becomes more efficient and ensures that the most effective configuration is identified to maximize the SVM's classification accuracy.

The purpose of tuning these hyperparameters is to identify the combination that provides the best balance between model complexity and generalization performance. A well-tuned model avoids overfitting, where it becomes too tailored to the training data and performs poorly on unseen data, while also avoiding underfitting, where the model is too simple to capture the underlying patterns in the data. By adjusting hyperparameters like C and the kernel type, the model can achieve optimal complexity, ensuring it generalizes well to new, unseen data and delivers accurate predictions. GridSearchCV systematically explores various combinations of hyperparameters to identify the best set that optimizes the model's performance. It does this by performing an exhaustive search over a specified grid of parameter values and evaluating the model's accuracy using cross-validation for each combination. The result is the selection of the hyperparameters that yield the highest performance, ensuring that the model is fine-tuned for maximum effectiveness in classification tasks. This approach helps to ensure that the model generalizes well to new, unseen data while achieving the best possible accuracy.

### 4. Results and Discussions:

Each image in the first sub-dataset, consisting of 367 images with a resolution of  $640 \times 480$ pixels, is used to classify one of four distinct types of white blood cells: neutrophils, eosinophils, lymphocytes, and monocytes. These images serve as the input for the classification task, with the goal of training a model to accurately differentiate between the different cell types based on their visual characteristics. The variety of cell types adds complexity to the classification task, requiring the model to learn and recognize subtle differences in appearance across the images. The third sub-dataset, known as ALL-IDB2, contains 260 images of lymphocytes, which are used for diagnosing acute lymphoblastic leukemia (ALL). These images are divided into two categories: mature and immature lymphocytes. Each image has a resolution of  $257 \times 257$  pixels. The purpose of this sub-dataset is to train and test models that can distinguish between mature and immature lymphocytes, which is a key step in diagnosing ALL and understanding the progression of the disease. Dataset 3 includes 200 red blood smear samples that were collected from a variety of websites and internet searches. These samples represent a diverse set of red blood cell images, which are typically used for tasks such as identifying abnormalities or classifying different blood cell types. The varied sources of the samples may introduce different imaging conditions, offering a broader range of examples for training and testing classification models. This dataset is essential for improving the robustness of models in recognizing red blood cells and detecting potential medical conditions.



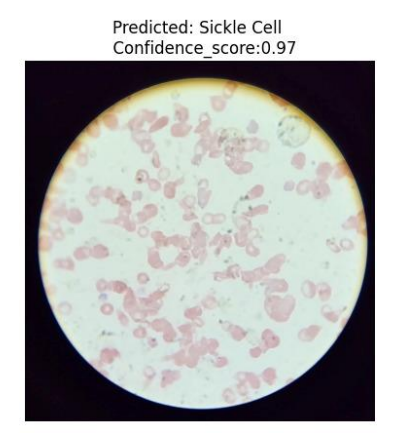


Figure 6: (a) Normal Confidence score (b) SCA predicted Confidence score

By using Dataset 1 as the target dataset, Dataset 2 for transfer learning, and Dataset 3 to demonstrate the robustness of the proposed models, the researchers achieved an impressive 99.98% accuracy with Model 2 under Scenario 4. This approach highlights the effectiveness of combining different datasets for training, fine-tuning, and evaluating models. Transfer learning from Dataset 2 likely enhanced Model 2's ability to generalize, while Dataset 3 served as a stress test, ensuring the model's robustness across diverse real-world data. This combination of strategies led to exceptionally high classification performance. In Scenario 4, the authors combine the strategies of transfer learning using Dataset 2 and data augmentation to enhance the performance of the model. Transfer learning allows the model to leverage pretrained knowledge from Dataset 2, while data augmentation increases the diversity of the training data by applying transformations such as rotations, flips, and scaling. This combination helps the model generalize better to new, unseen data and improves its robustness, ultimately contributing to the outstanding 99.98% accuracy achieved with Model 2 in this scenario. This approach begins with the transfer learning step, where the models are first trained on Dataset 2. To enhance the model's ability to recognize a wide variety of blood cell types, Dataset 2 is augmented with additional images. This data augmentation helps diversify the dataset by introducing variations such as rotations, scaling, and flips, which boosts the model's capacity to generalize across different appearances and conditions of the blood cells. By training on this augmented version of Dataset 2, the model gains a more robust understanding of the characteristics of different blood cells before being fine-tuned on the target Dataset 1. By leveraging the knowledge gained from this initial phase, the models are already equipped with a strong foundation in recognizing different blood components.

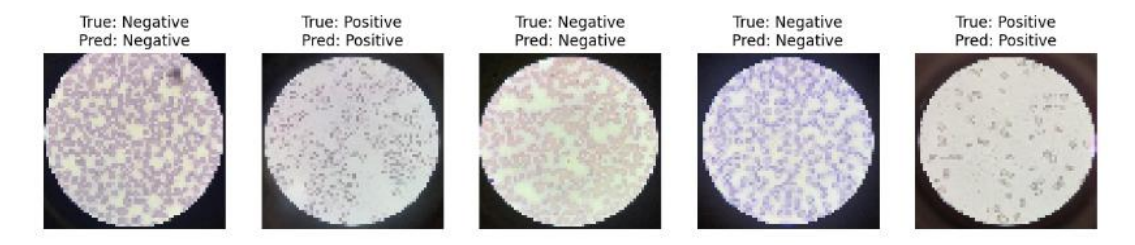


Figure 7: Positive and Negative predictions of SCA

Nanotechnology Perceptions Vol. 20 No.5 (2024)

After the initial transfer learning phase using Dataset 2, the authors introduce augmented images into the training process to further enhance the model's ability to generalize. This step involves applying various augmentation techniques such as flipping, rotating, and scaling to the images, effectively increasing the variability of the data. The introduction of augmented images ensures that the model is exposed to a wider range of possible image variations, improving its robustness and enabling it to handle more diverse and complex real-world scenarios. By combining transfer learning with data augmentation, the model becomes more adept at recognizing blood components across different conditions. The augmented images include variations of the original images, created through techniques such as rotation, flipping, and brightness adjustments. These transformations introduce new perspectives and subtle changes to the images, allowing the model to learn from a more diverse set of examples. This helps the model become more adaptable, as it can better recognize blood components under different orientations, lighting conditions, and other real-world variations. The use of such data augmentation techniques plays a crucial role in improving the model's generalization ability, especially when faced with unseen data during testing.

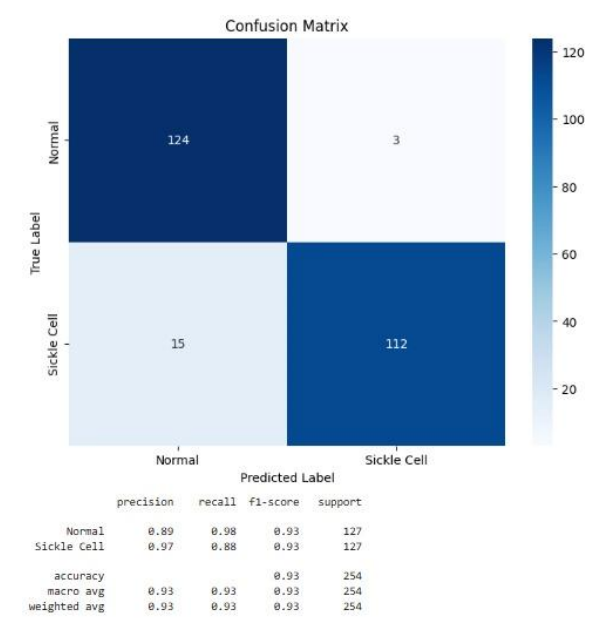


Figure 12: Confusion Matrix

By combining the transferred knowledge from Dataset 2 with the augmented data, the authors were able to achieve exceptional results. During the model training, the ResNet-50 model reached a remarkable 100% accuracy when trained on a dataset consisting of 5000 augmented images. The combination of transfer learning and data augmentation allowed the model to learn more generalized and robust features, ensuring that it could effectively classify a wide variety of blood cell types. The 100% accuracy achieved highlights the power of this approach, showcasing how leveraging pre-trained models and enhancing the dataset with augmented images can lead to outstanding performance. For a more comprehensive investigation, this research extended the dataset size to include 10,002 images. By increasing the number of images, the researchers were able to further improve the model's ability to generalize and

ensure that it could handle a larger variety of data, making the model more robust and better suited for real-world applications. The larger dataset also helps to provide a more thorough evaluation of the model's performance, reducing the risk of overfitting and giving a more accurate representation of how the model will perform on unseen data. It is essential to emphasize that the dataset used in this research differs from the one employed by Alzubaidi et al., highlighting the importance of this distinction in terms of dataset composition and size. While both datasets may share similarities in terms of the types of images used, the size and variety of the dataset in this study offer a broader and potentially more diverse set of examples for training and evaluation. This difference in dataset characteristics plays a significant role in the generalization and performance of the model, making the findings in this research particularly noteworthy in comparison to previous studies.

Model Accuracy Precision Recall F1 Score VGG19-BN-CNN 92.4 96.2 Hybrid 97.2 95.2 (Proposed) ResNet50 93.2 93.9 92.6 93.2 InceptionV3 91.9 92.3 91.1 91.7 MobileNetV2 89.4 90.2 88.6 89.4 Custom CNN 86.8 87.4 85.6 86.5

Table 3: Performance Measures

Furthermore, it is worth noting that this research yielded highly competitive results. These impressive results were obtained using the augmented erythrocytesIDB dataset, which contained 10,002 images. The high accuracy achieved by both model combinations demonstrates the effectiveness of the approach, highlighting how leveraging transfer learning, data augmentation, and well-chosen classifiers can lead to exceptional performance in the classification of blood cells.

The parameters were carefully set after running multiple experiments and observing the behavior of the models. To ensure consistency and fairness in comparison, all the models used the same batch size, learning rate, optimizer, and dropout regularization. By maintaining these hyperparameters across all models, the researchers ensured that the performance differences observed were due to the model architecture and not influenced by variations in training configurations. This approach allowed for a more controlled evaluation of the models' effectiveness in the classification task.

### 5. Conclusion:

This study presents an approach for classifying Sickle Cell Disease (SCD), focusing on multiclass classification to distinguish between three categories: circular (normal red blood cells), elongated (sickle-shaped cells), and other (non-circular and non-elongated cell shapes). To assess the effectiveness of the model, various metrics are used, including a confusion matrix, accuracy, precision, recall, and F1-measure values. The perfect performance metrics indicate that the model has successfully learned to identify the key features associated with each cell type, making it highly reliable for Sickle Cell Disease classification tasks. Similarly,

the AlexNet model demonstrated balanced performance, achieving 98% precision and 99% recall for circular and elongated shapes. This indicates that while AlexNet may not have reached the perfect scores of ResNet-50, it still delivered strong and reliable results for these cell categories. MobileNet also exhibited competitive metrics, showcasing its ability to perform well in the classification task despite being a more lightweight model. These results emphasize the versatility of different architectures in achieving high performance for Sickle Cell Disease classification, with each model demonstrating strengths in various aspects of the evaluation metrics. The experimental results in this study demonstrate significant performance enhancements across multiple models. Each model, from ResNet-50 to AlexNet and MobileNet. showed improvements in classification accuracy, precision, recall, and F1-score, reflecting the effectiveness of the approach. The use of transfer learning, data augmentation, and well-optimized model architectures contributed to these performance gains, enabling the models to better distinguish between different cell shapes and ultimately achieve higher classification accuracy. This result highlights the model's effectiveness despite being a lightweight architecture, designed to optimize performance while minimizing computational costs. The high accuracy of MobileNetV2 demonstrates its ability to perform well on the Sickle Cell Disease classification task, making it an excellent choice for applications where efficiency and accuracy are both important. This performance also reflects the model's capability to generalize effectively, even with the constraints of a smaller, more resource-efficient architecture. Subsequently, the integration of the ablation experiment, which combined the Random Forest (RF) classifier with the MobileNetV2 model, yielded an even higher accuracy of 97.29%. This result signifies a substantial increase of 0.3% over the original MobileNetV2 model's performance. The addition of the RF classifier helped improve the model's decisionmaking process by leveraging the strengths of both deep learning and traditional machine learning techniques. This significant boost highlights the effectiveness of integrating deep learning with support vector machines, leveraging SVM's strong classification capabilities alongside the feature extraction power of MobileNetV2. The combination resulted in a highly accurate model for classifying Sickle Cell Disease, further demonstrating the potential of hybrid models in achieving exceptional performance on complex classification tasks. By leveraging SVM's ability to find optimal decision boundaries, the combined model achieved even higher accuracy, further solidifying its potential for accurate and reliable classification of Sickle Cell Disease. This improvement demonstrates how integrating deep learning and traditional machine learning techniques can lead to superior results in complex classification tasks. Notably, the methods and models employed in this research—such as the deep transfer learning models, hyper parameter tuning, ablation experiment, and dataset augmentation outperformed other novel approaches that primarily focused on machine learning and related techniques for Sickle Cell Disease. The integration of deep transfer learning allowed the models to leverage pre-trained knowledge, significantly improving performance. Hyperparameters tuning ensured optimal model configuration, while the ablation experiment demonstrated the value of combining different techniques like deep learning with traditional machine learning classifiers. Additionally, augmenting the dataset enhanced the model's generalization ability, providing a more robust and comprehensive solution to Sickle Cell Disease classification compared to approaches that relied solely on traditional machine learning methods.

## References

- H. Frangoul, D. Altshuler, M.D. Cappellini, Y.-S. Chen, J. Domm, B.K. Eustace, J. Foell, J. de la Fuente, S. Grupp, R. Handgretinger, T.W. Ho, A. Kattamis, A. Kernytsky, J. Lekstrom-Himes, A.M. Li, F. Locatelli, M.Y. Mapara, M. de Montalembert, D. Rondelli, A. Sharma, S. Sheth, S. Soni, M.H. Steinberg, D. Wall, A. Yen, S. Corbacioglu, CRISPR-Cas9 gene editing for sickle cell disease and βthalassemia, N. Engl. J. Med. 384 (2021) 252–260, https://doi.org/10.1056/nejmoa2031054.
- 2. G.J. Kato, F.B. Piel, C.D. Reid, M.H. Gaston, K. Ohene-Frempong, L. Krishnamurti, W.R. Smith, J.A. Panepinto, D.J. Weatherall, F.F. Costa, E.P. Vichinsky, Sickle cell disease, Nat. Rev. Dis. Prim. 4 (2018) 1–22, https://doi.org/10.1038/nrdp.2018.10.
- D. Iskander, G. Wang, E.F. Heuston, C. Christodoulidou, B. Psaila, K. Ponnusamy, H. Ren, Z. Mokhtari, M. Robinson, A. Chaidos, P. Trivedi, N. Trasanidis, A. Katsarou, R. Szydlo, C.G. Palii, M.H. Zaidi, Q. Al-Oqaily, V.S. Caputo, A. Roy, Y. Harrington, L. Karnik, K. Naresh, A.J. Mead, S. Thongjuea, M. Brand, J. de la Fuente, D.M. Bodine, I. Roberts, A. Karadimitris, Single-cell profiling of human bone marrow progenitors reveals mechanisms of failing erythropoiesis in Diamond-Blackfan anemia, Sci. Transl. Med. 13 (2021), https://doi.org/10.1126/SCITRANSLMED.ABF0113/SUPPL\_FILE/SCITRANSLMED.ABF0113\_DATA\_FILES\_S1\_TO\_S6.ZIP.
- 4. A.M. Taylor, E.R. Macari, I.T. Chan, M.C. Blair, S. Doulatov, L.T. Vo, D.M. Raiser, K. Siva, A. Basak, M. Pirouz, A.N. Shah, K. McGrath, J.M. Humphries, E. Stillman, B.P. Alter, E. Calo, R.I. Gregory, V.G. Sankaran, J. Flygare, B.L. Ebert, Y. Zhou, G.Q. Daley, L.I. Zon, Calmodulin inhibitors improve erythropoiesis in Diamond-Blackfan anemia, Sci. Transl. Med. 12 (2020), https://doi.org/10.1126/SCITRANSLMED.ABB5831/SUPPL\_FILE/ABB5831\_SM.PDF.
- Y. Zhang, Y. Dai, J. Wen, W. Zhang, A. Grenz, H. Sun, L. Tao, G. Lu, D.C. Alexander, M.V. Milburn, L. Carter-Dawson, D.E. Lewis, W. Zhang, H.K. Eltzschig, R. E. Kellems, M.R. Blackburn, H.S. Juneja, Y. Xia, Detrimental effects of adenosine signaling in sickle cell disease, Nat. Med. 171 (17) (2010) 79–86, https://doi.org/10.1038/nm.2280, 2010.
- 6. E.B. Esrick, L.E. Lehmann, A. Biffi, M. Achebe, C. Brendel, M.F. Ciuculescu, H. Daley, B. MacKinnon, E. Morris, A. Federico, D. Abriss, K. Boardman, R. Khelladi, K. Shaw, H. Negre, O. Negre, S. Nikiforow, J. Ritz, S.-Y. Pai, W.B. London, C. Dansereau, M.M. Heeney, M. Armant, J.P. Manis, D.A. Williams, Posttranscriptional genetic silencing of BCL11A to treat sickle cell disease, N. Engl. J. Med. 384 (2021) 205–215, https://doi.org/10.1056/nejmoa2029392.
- M. Eapen, R. Brazauskas, M.C. Walters, F. Bernaudin, K. Bo-Subait, C.D. Fitzhugh, J.S. Hankins, J. Kanter, J.J. Meerpohl, J. Bola nos-Meade, J.A. Panepinto, D. Rondelli, S. Shenoy, J. Williamson, T.L. Woolford, E. Gluckman, J.E. Wagner, J.F. Tisdale, Effect of donor type and conditioning regimen intensity on allogeneic transplantation outcomes in patients with sickle cell disease: a retrospective multicentre, cohort study, Lancet Haematol 6 (2019) e585–e596, https://doi.org/10.1016/S2352-3026(19)30154-1.
- 8. M.R. DeBaun, L.C. Jordan, A.A. King, J. Schatz, E. Vichinsky, C.K. Fox, R.C. McKinstry, P. Telfer, M.A. Kraut, L. Daraz, F.J. Kirkham, M.H. Murad, American Society of Hematology 2020 guidelines for sickle cell disease: prevention, diagnosis, and treatment of cerebrovascular disease in children and adults, Blood Adv 4 (2020) 1554–1588, https://doi.org/10.1182/bloodadvances.2019001142.
- 9. M.Z. Alom, T.M. Taha, C. Yakopcic, S. Westberg, P. Sidike, M.S. Nasrin, M. Hasan, B.C. Van Essen, A.A.S. Awwal, V.K. Asari, A state-of-the-art survey on deep learning theory and architectures, Electron 8 (2019), https://doi.org/10.3390/electronics8030292.
- 10. S. Deepak, P.M. Ameer, Brain tumor classification using deep CNN features via transfer learning, Comput. Biol. Med. 111 (2019), 103345, https://doi.org/10.1016/j.compbiomed.2019.103345.
- 11. A. Ardakani, A.R. Kanafi, U.R. Acharya, N. Khadem, A. Mohammadi, Application of deep learning technique to manage COVID-19 in routine clinical practice using CT images: results of 10 convolutional neural networks, Comput. Biol. Med. 121 (2020), 103795, https://doi.org/10.1016/j.compbiomed.2020.103795.
- 12. H. Kutlu, E. Avci, F. "Ozyurt, White blood cells detection and classification based on regional convolutional neural networks, Med. Hypotheses 135 (2020), 109472,

- https://doi.org/10.1016/j.mehy.2019.109472.
- 13. A. Krizhevsky, I. Sutskever, G.E. Hinton, ImageNet classification with deep convolutional neural networks, Commun. ACM 60 (2017) 84–90, https://doi.org/10.1145/3065386.
- K. Simonyan, A. Zisserman, Very deep convolutional networks for large-scale image recognition, 3rd
   Int. Conf. Learn. Represent. ICLR 2015 Conf. Track Proc. (2015) 1–14.
- 15. C. Szegedy, W. Liu, Y. Jia, P. Sermanet, S. Reed, D. Anguelov, D. Erhan, V. Vanhoucke, A. Rabinovich, Going deeper with convolutions, IEEE Comput. Soc. Conf. Comput. Vis. Pattern Recogn. (2015) 1–9, https://doi.org/10.1109/CVPR.2015.7298594, 07-12-June.
- 16. P.K. Das, S. Meher, R. Panda, A. Abraham, A review of automated methods for the detection of sickle cell disease, IEEE Rev. Biomed. Eng. (2020), https://doi.org/10.1109/RBME.2019.2917780.
- 17. H.F. Bunn, Pathogenesis and treatment of sickle cell disease, N. Engl. J. Med. (1997), https://doi.org/10.1056/nejm199709113371107.
- 18. F.B. Piel, A.P. Patil, R.E. Howes, O.A. Nyangiri, P.W. Gething, M. Dewi, W.H. Temperley, T.N. Williams, D.J. Weatherall, S.I. Hay, Global epidemiology of Sickle haemoglobin in neonates: a contemporary geostatistical model-based map and population estimates, Lancet (2013), https://doi.org/10.1016/S0140-6736(12)61229-X.
- 19. F.O. Ortiz, T.K. Aldrich, R.L. Nagel, L.J. Benjamin, Accuracy of pulse oximetry in sickle cell disease, Am. J. Respir. Crit. Care Med. (1999), https://doi.org/10.1164/ajrccm.159.2.9806108.
- 20. N. Petrovi c, G. Moy`a-Alcover, A. Jaume-i-Cap´o, M. Gonz´alez-Hidalgo, Sickle-cell disease diagnosis support selecting the most appropriate machine learning method: towards a general and interpretable approach for cell morphology analysis from microscopy images, Comput. Biol. Med. 126 (2020), https://doi.org/10.1016/j.compbiomed.2020.104027.
- M. Darrin, A. Samudre, M. Sahun, S. Atwell, C. Badens, A. Charrier, E. Helfer, A. Viallat, V. Cohen-Addad, S. Giffard-Roisin, Classification of red cell dynamics with convolutional and recurrent neural networks: a sickle cell disease case study, Sci. Rep. 13 (2023) 1–12, https://doi.org/10.1038/s41598-023-27718-w.
- D. Maxime, S. Ashwin, S. Maxime, A. Scott, B. Catherine, C. Anne, H. Emmanuele, V. Annie, C.-A. Vincent, G.-R. Sophie, Classification of Blood Cells Dynamics with Convolutional and Recurrent Neural Networks: a Sickle Cell Disease Case Study, 2021, https://doi.org/10.5281/ZENODO.5723606.
- 23. C. Patgiri, A. Ganguly, Adaptive thresholding technique based classification of red blood cell and sickle cell using Naïve Bayes Classifier and K-nearest neighbor classifier, Biomed. Signal Process Control 68 (2021), 102745, https://doi.org/10.1016/j.bspc.2021.102745.
- K.M. Hosny, M.A. Kassem, M.M. Fouad, Classification of skin lesions into seven classes using transfer learning with AlexNet, J. Digit. Imag. 33 (2020) 1325–1334, https://doi.org/10.1007/s10278-020-00371-9.
- 25. H. Ismail Fawaz, B. Lucas, G. Forestier, C. Pelletier, D.F. Schmidt, J. Weber, G.I. Webb, L. Idoumghar, P.A. Muller, F. Petitjean, InceptionTime: finding AlexNet for time series classification, Data Min. Knowl. Discov. 34 (2020) 1936–1962, https://doi.org/10.1007/s10618-020-00710-y.
- 26. G. Jacob, R.T. Pramod, H. Katti, S.P. Arun, Qualitative similarities and differences in visual object representations between brains and deep networks, Nat. Commun. 121 (12) (2021) 1–14, https://doi.org/10.1038/s41467-021-22078-3, 2021.
- 27. A. Victor Ikechukwu, S. Murali, R. Deepu, R.C. Shivamurthy, ResNet-50 vs VGG-19 vs training from scratch: a comparative analysis of the segmentation and classification of Pneumonia from chest X-ray images, Glob. Transitions Proc. 2 (2021) 375–381, https://doi.org/10.1016/j.gltp.2021.08.027.